# Local Structure and Dynamics in Solvent-Swollen Polymers

**Florian Müller-Plathe***

*Laboratorium für Physikalische Chemie, Eidgenössische Technische Hochschule Zürich, ETH Zentrum, CH-8092 Zürich, Switzerland*

*Received December 19, 1995; Revised Manuscript Received April 11, 1996*[⊗]

ABSTRACT: We report atomistically detailed molecular dynamics simulations of benzene−polystyrene systems (0−84.2 wt % polystyrene). We have calculated solvent diffusion coefficients and have found that their composition dependence not only shows good agreement with experiment but also follows quite well the predictions by lattice models. We also show that, for the polystyrene−benzene system studied here, it is not possible to separate solvent molecules into slow ones, tightly bound to the polymer, and fast ones, not bound to the polymer. This would suggest that, in a gel, the polymer chains alone act as obstacles to solvent diffusion and not polymer decorated by a shell of solvent molecules. We have found the reorientation of benzene molecules in the gel to be nonexponential and anisotropic, the reorientation of the ring normal being slower than the in-plane reorientation. This anisotropy increases dramatically with polystyrene concentration. At the highest polymer concentration, the time scales for the two motions are separated by 3 orders of magnitude. The changes of polymer solvation and polymer dynamics with concentration are discussed. For all polymer concentrations above 50 wt %, the polymer turns out to be essentially rigid on a nanosecond time scale with only local fluctuations possible.

## 1. Introduction

Many synthetic polymers are swollen by suitable solvents, some to the degree of dissolution if there is sufficient solvent available. Solvent uptake not only significantly alters the polymer properties but often is the first step in a deterioration or degradation process that ultimately renders the polymer useless.[1] On the other hand, there are polymer applications (e.g. in pervaporation, ion exchange, electrodialysis, disposable nappies) which rely on the polymer to be at least partially swollen. The understanding of the mechanism of solvent uptake and solvent-induced swelling is therefore of practical interest. In addition, polymer−solvent systems are interesting model systems for solvent behavior in restricted geometries, since they can be easily modified to provide a wide variety of boundary conditions to diffusants. Networks can be generated by cross-linking, mesh sizes can be changed via the cross-link density, and the stiffness of the polymer chains can be varied by altering their chemical composition as can be the strength of the polymer−solvent interaction. Finally, solvent can be used as a spectroscopic probe to shed light on the dynamics of the polymer itself.[2−5]

Mixtures of polystyrene (PS) and numerous solvents have been studied experimentally. Berens and Hopfenberg have measured diffusion coefficients of trace concentrations of solvent in PS and related them to solvent diameters.[6] Kosfeld and Goffloo[7] as well as Blum et al.[8,9] have obtained solvent diffusion coefficients at PS concentrations of 0−85 wt % from pulsed-gradient-spin-echo NMR data and used them to test various theoretical predictions. Sillescu and co-workers have measured by NMR translational diffusion coefficients of toluene in PS[10] and rotational diffusion times for neat toluene at low temperatures.[11] The rotation of Aroclor (a mixture of polychlorinated biphenyls) in PS has been studied by both depolarized Rayleigh scattering and photon correlation spectroscopy.[12,13]

Molecular simulation and, in particular, molecular dynamics (MD) have, in the past few years, made important contributions to the understanding of the behavior of small molecules inside bulk polymers. Most of these studies have involved gas molecules at low concentrations in amorphous polymers (for reviews, see refs 14 and 15). Computational studies have recently been extended to low concentrations of $H_2O$ and ethanol in poly(dimethylsiloxane),[16] gas molecules ($CH_4$ and $CO_2$) in *crystalline* rather than amorphous poly(4-methylpentene),[17] and poly(ethylene oxide)-based polymer electrolytes.[18−20] Polymer-solvent systems, on the other hand, have so far been investigated computationally only in the dilute-solution limit, i.e. one polymer molecule in an excess of solvent molecules (for example, poly(ethylene oxide) in benzene[21] or polyisoprene in toluene[22]).

In the present contribution, we extend the MD approach to polymer−solvent systems in the gray area of intermediate concentrations, that is, between the well-investigated single-molecule-in-bulk-polymer limit and the equally well-investigated single-polymer-in-bulk-solvent limit. We believe that there are interesting phenomena to be found at polymer concentrations of 10−90 wt %. As a first application, we chose the system of polystyrene and benzene for which simulation parameters are easily found, and which, at the same time, is close to the well-characterized PS−toluene system. Both benzene[21,23−26] and PS[27−31] have previously been studied—separately—by simulation.

## 2. Model and Simulation Details

Simulations were carried out for systems of pure benzene and polystyrene as well as of mixtures. The potential energy function is defined in Table 1. For benzene, we used the nonbonded parameters of Jorgensen and Severance.[26] These have been adjusted to reproduce the experimental density (at 1 atm) and heat of vaporization of liquid benzene. This all-atom model has small partial charges on the carbon and hydrogen atoms in order to reproduce the electric quadrupole moment of the benzene molecule. The values of the charges were confirmed by our own ab initio calculations.[32] Since our molecular dynamics program does not handle completely rigid molecules, we augmented the benzene force field by bond angle bending and harmonic dihedral terms, bond distances being held fixed by

* Present address: Max-Planck-Institut für Polymerforschung, D-55128 Mainz, Germany.

[⊗] Abstract published in *Advance ACS Abstracts,* May 15, 1996.

S0024-9297(95)01876-6 CCC: $12.00 

**Table 1. Potential Energy Function Parameters**[a]

| nonbonded interactions[b] | $V(r_{ij}) = 4\epsilon[(\sigma/r_{ij})^{12} - (\sigma/r_{ij})^6] + q_i q_j/4\pi\epsilon_0 r_{ij}$ | | |
|---|---|---|---|
| | $\epsilon$/kJ mol$^{-1}$ | $\sigma$/nm | $q$/e |
| $C_{ali}$ | 0.3519 | 0.3207 | 0 |
| $H_{ali}$ | 0.318 | 0.2318 | 0 |
| $C_{aro}$ | 0.294 | 0.355 | −0.115[c] |
| $H_{aro}$ | 0.126 | 0.242 | +0.115 |

| bond | distance/nm |
|---|---|
| $C_{ali}-C_{ali}$ | 0.153 |
| $C_{ali}-H_{ali}$ | 0.11 |
| $C_{aro}-C_{aro}$ | 0.139 |
| $C_{aro}-H_{aro}$ | 0.108 |
| $C_{ali}-C_{aro}$ | 0.151 |

| bond angles | $V(\phi) = (k_\phi/2)(\phi - \phi_0)^2$ | |
|---|---|---|
| | $\phi_0$ /deg | $k_\phi$ /kJ mol$^{-1}$ rad$^{-2}$ |
| $H-C_{ali}-H$ | 109.45 | 306.4 |
| $C_{ali}-C_{ali}-H$ | 109.45 | 366.9 |
| $C_{ali}-C_{ali}-C_{ali}$ | 109.45 | 482.3 |
| $C_{aro}-C_{ali}-H$ | 109.45 | 366.9 |
| $C_{ali}-C_{ali}-C_{aro}$ | 109.45 | 482.3 |
| $C_{ali}-C_{aro}-C_{aro}$ | 120.0 | 376.6 |
| $C_{aro}-C_{aro}-C_{aro}$ | 120.0 | 376.6 |
| $C_{aro}-C_{aro}-H$ | 120.0 | 418.8 |

| dihedral angles | $V(\tau) = (k_\tau/2)[1 - \cos 3(\tau - \tau_0)]$, *cis* at 0° | | |
|---|---|---|---|
| | $\tau_0$/deg | $k_\tau$/kJ mol$^{-1}$ | |
| $C_{ali}-C_{ali}-C_{ali}-C_{ali}$ | 180.0 | 12.0 | |
| $C_{ali}-C_{ali}-C_{ali}-H$ | 180.0 | 12.0 | (terminal methyl) |

| harmonic dihedral angles | $V(\delta) = (k_\delta/2)(\delta - \delta_0)^2$, *cis* at 0° | |
|---|---|---|
| | $\delta_0$ /deg | $k_\delta$ /kJ mol$^{-1}$ rad$^{-2}$ |
| $C_{aro}-C_{aro}-C_{aro}-C_{aro}$ | 0.0 | 167.4 |
| $C2_{aro}-C3_{aro}-C1_{aro}-H$[on C2] | 0.0 | 167.4 |
| $C2_{aro}-C3_{aro}-C1_{aro}-C_{ali}$[on C2] | 0.0 | 167.4 |

[a] The subscripts ali and aro denote aliphatic and aromatic atoms, respectively. [b] Nonbonded interactions are excluded between first and second neighbors. In addition, nonbonded interactions between all atoms of a given benzene molecule or phenyl group are excluded. [c] The charge on carbon 1 of the phenyl group in polystyrene is 0.

constraints. The phenyl groups of polystyrene were described by the same parameters as the benzene molecules. Parameters for aliphatic carbon and hydrogen were those we used before for aliphatic polymers.[17] They are very close to parameters derived using the Slater−Kirkwood rules.[30] Parameters for unlike interactions were determined using the Lorentz−Berthelot mixing rules.[33] A barrier height of 12 kJ/mol was adopted for the rotation of polystyrene backbone dihedral angles following ab initio (HF/6-31G**) calculations on polystyrene fragments (not shown). No special potential was imposed on the rotation of the phenyl rings, since steric hindrance dominates the barrier to phenyl ring flips, and this is explicitly included.

An atactic random polystyrene chain of 100 monomers was generated in vacuum using the rotational isomeric state theory weights of ref 30. It consisted of 46% meso dyads. Subsequently, this chain was placed into a cubic periodic simulation cell at a reduced density of about 500 kg/m$^3$. The cell was then filled with 106 benzene molecules in random configurations resulting in a final density of ∼1000 kg/m$^3$. At this preparatory stage, no care was taken to avoid atom overlaps. The system was then energy-minimized to remove the worst close contacts. Energy minimization, however, still left some polymer entanglements, polymer chains poking through benzene rings and so on. All of this was efficiently removed by a 50 ps molecular dynamics run using soft-core potentials. Soft-core potentials have been newly implemented in our simulation program YASP[34] in the following way. The short-range part (0−0.35 nm, e.g.) of the nonbonded potential energy function is replaced by a cubic spline. The spline coefficients are chosen to satisfy four conditions: the spline matches the value (i) and the derivative (ii) of the original potential energy function at the crossover distance; its derivative is zero at an interatomic distance $r$ of zero (iii); most importantly, its value $V_0$ at $r = 0$ is finite (iv). This gets rid of the singularity at $r = 0$ and allows atoms to pass through each other. We typically start these relaxation simulations with $V_0 = 4k_BT$ (≈10 kJ/mol at 300 K) and increase $V_0$ stepwise to 20 or 50 $k_BT$, before turning to simulations with the full potential. These calculations were initially done at constant $NPT$ coupling the $x$, $y$, and $z$ lengths of the simulation box separately to a pressure bath of 1 atm. This allowed the simulation box to distort slightly from cubic to orthorhombic. After 100 ps, the aspect ratio was frozen and the box volume as a whole was coupled to the isotropic pressure for the remaining simulations.

Systems with fewer than 106 benzene molecules (see also Table 2) were generated by successively deleting appropriate numbers of benzene molecules from configurations taken out of production runs, and letting the system relax to its new equilibrium density. The system with 212 benzene molecules was generated from a configuration of the 106 benzene system by duplicating each benzene, offsetting it from its parent by 0.1 nm in the $x$ direction, and rerunning the procedure of energy minimization, soft-core dynamics, and $NPT$ dynamics to reach the final density. The system of pure benzene was generated by placing the centers of mass of the benzene molecules on a periodic diamond lattice and relying on standard $NPT$ dynamics for it to relax to a liquid structure. For all systems, the end of equilibration was assumed as soon as the density did not change anymore. Equilibration and sampling times are listed in Table 2.

Table 2 also provides the interconversion of the various concentration units. One measure of concentration is the polymer volume fraction Φ. This quantity is readily defined for lattice models, but its microscopic definition is ambiguous for continuous models. We calculated from one configuration near the end of the simulation of each of the systems the volume occupied by the polymer and by the solvent, respectively. This is done by randomly picking points in the simulation cell and counting the points within the Lennard-Jones radius of any polymer atom (polymer volume) or any solvent atom (solvent volume) or outside any atomic radius (free volume). The radius of an atom is taken as half its $\sigma$ parameter (Table 1). The polymer volume fraction Φ is then defined as the polymer volume divided by the sum of the polymer and solvent volumes. By disregarding the free volume, this definition effectively assumes that the free volume is proportionally distributed among the polymer and the solvent.

Molecular dynamics was run at constant temperature $T$ and constant pressure $P$, by weak coupling[35] to a temperature bath of 300 K and a pressure bath of 101.3 kPa. The coupling times were 0.2 ps ($T$) and 0.5 ps ($P$). The time step was 2 fs. All bond lengths were constrained using the SHAKE algorithm[36,37] with a relative tolerance of $10^{-7}$. For nonbonded interactions, a cutoff

**Table 2. System Composition**

| no. of benzene molecules | no. of styrene monomers | wt % polystyrene | vol fraction polystyrene $\Phi$[a] | simulation time (ns): equilibration/production |
|---|---|---|---|---|
| 215 | 0 | 0 | 0 | 0.05/0.334 |
| 212 | 100 | 38.6 | 0.36 | 0.16/0.6 |
| 106 | 100 | 55.7 | 0.57 | 1.35/3.54 |
| 50 | 100 | 72.7 | 0.78 | 2.0/1.6 |
| 25 | 100 | 84.2 | 0.84 | 2.75/7.4 |

[a] For the definition of $\Phi$, see text.

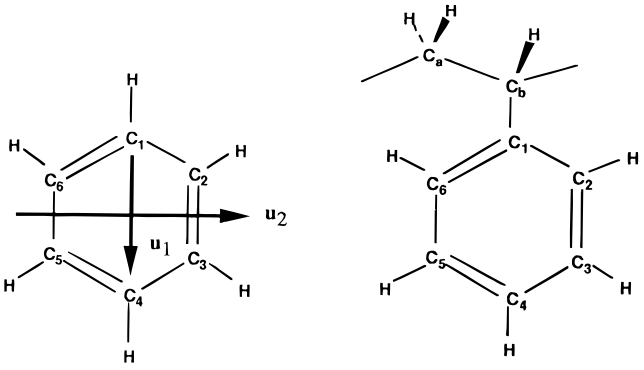


**Figure 1.** Atom labeling and orientation vectors for benzene and polystyrene.

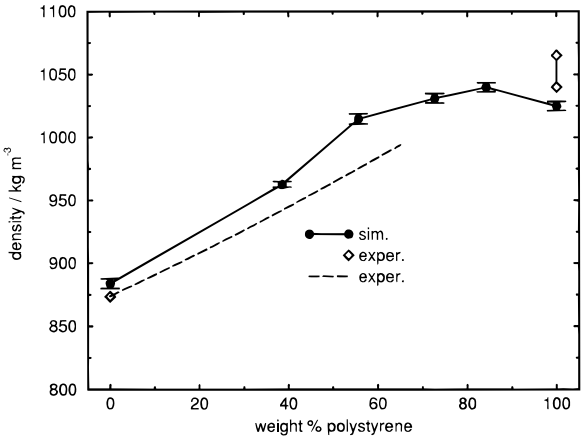


**Figure 2.** Calculated mass densities of benzene−polystyrene mixtures at 300 K and 101.3 kPa. The error bars denote the root-mean-square fluctuations of the density. Experimental data[39,40,42] are included for reference.

distance of 1.0 nm was used, with a reaction-field correction for the Coulombic interactions;[34] the effective dielectric constant of the continuum $\epsilon_{RF}$ was taken to be 2.5 (experimental dielectric constants: 2.3 for liquid benzene, ≈2.5 for amorphous PS). An atomic Verlet neighbor list was used, which was updated every 15 time steps; neighbors were included if they were closer than 1.1 nm. Configurations were saved every 1 ps.

From the trajectories, the center-of-mass mean-square displacement (MSD)

$$\mathrm{MSD} = \langle|\mathbf{R}(t) - \mathbf{R}(0)|^2\rangle$$

and the center-of-mass mean-square fluctuation (MSF)

$$\mathrm{MSF} = \langle|\mathbf{R}(t) - \bar{\mathbf{R}}|^2\rangle$$

were calculated. A benzene's center of mass position at time $t$ is denoted by $\mathbf{R}(t)$, its average position, by $\bar{\mathbf{R}}$. Angle brackets imply ensemble averaging which, in our simulations, is realized by averaging over different molecules, as well as over time origins. Both quantities are time-dependent. In the long-time limit of normal (Einstein) diffusion,[38] they increase linearly with time, and a diffusion coefficient $D$ can be calculated from the slope of either of them.

$$D = \frac{1}{6}\lim_{t\to\infty}\frac{\mathrm{d}}{\mathrm{d}t}\langle|\mathbf{R}(t) - \mathbf{R}(0)|^2\rangle = \lim_{t\to\infty}\frac{\mathrm{d}}{\mathrm{d}t}\langle|\mathbf{R}(t) - \bar{\mathbf{R}}|^2\rangle$$

We find that, generally, diffusion coefficients calculated in both ways agree to within a few percent.

The rotation of a benzene molecule can be characterized by the time evolution of certain molecule-fixed unit vectors. They are illustrated in Figure 1. We arbitrarily take as unit vector $\mathbf{u}_1$ the in-plane vector from $C_1$ in the direction of $C_4$. The other in-plane vector $\mathbf{u}_2$, which is perpendicular to $\mathbf{u}_1$, is symmetrically equivalent ($\mathbf{u}_1$ and $\mathbf{u}_2$ together form a degenerate representation of the molecular point group) and contains no new information. A third orientation vector $\mathbf{u}_3$ is given by the ring normal $\mathbf{n}$. This we calculate as the appropriately normalized arithmetic mean of the normals of the two planes defined by atoms $C_1$, $C_3$, and $C_5$ and $C_2$, $C_4$, and $C_6$, respectively.

For any of the orientation vectors, we can calculate a time correlation function

$$\langle\cos\phi\rangle = \langle\mathbf{u}(t)\cdot\mathbf{u}(0)\rangle$$

This correlation function describes by what angle $\phi$, on average, $\mathbf{u}$ has rotated at time $t$, given that it was in position $\mathbf{u}(0)$ at time $t = 0$. Again, ensemble averaging is accomplished through averaging over both molecules and time origins. For molecular liquids, these correlation functions are often found to follow an exponential decay after some short-time features. We have found that the correlation functions in our polymer−solvent system are better fitted by stretched-exponential or Kohlrausch−Williams−Watts (KWW) functions

$$\langle\mathbf{u}(t)\cdot\mathbf{u}(0)\rangle \approx \exp[-(t/\alpha)^\beta]$$

A correlation time $\tau$ characteristic of the particular reorientation can be calculated as the time integral of the correlation function, which in the case of a stretched exponential is analytical,

$$\tau = \int_0^\infty \exp[-(t/\alpha)^\beta]\,\mathrm{d}t = \frac{\alpha}{\beta}\Gamma\left(\frac{1}{\beta}\right)$$

The motions leading to reorientation of $\mathbf{u}_1$ and $\mathbf{u}_3$ are also referred to in the literature as spinning and tumbling, respectively. The corresponding correlation times $\tau_1$ and $\tau_3$ have also been denoted as $\tau_\parallel$ and $\tau_\perp$, respectively.

## 3. Results and Discussion

**3.1. Bulk Properties.** The mass density of the benzene−polystyrene mixtures is shown in Figure 2. The density of neat benzene is well reproduced (calcu-

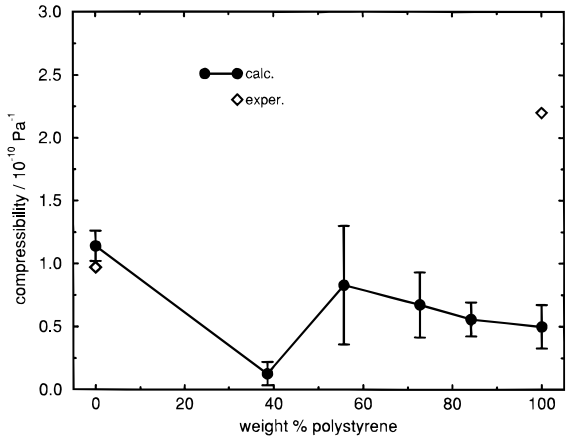


**Figure 3.** Isothermal compressibility of benzene−polystyrene mixtures at 300 K and 101.3 kPa, calculated from volume fluctuations. The error bars denote standard deviations between different subsections of the trajectory. Experimental data[39,42] are included for reference.

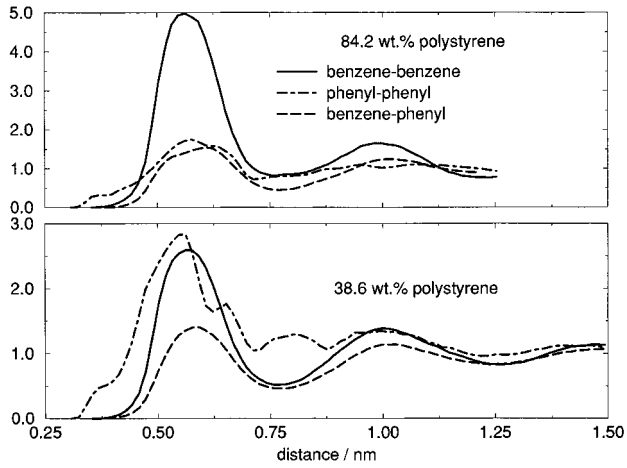


**Figure 4.** Center-of-mass radial distribution functions for aromatic groups (benzene and/or phenyl) for two benzene−polystyrene mixtures. The normalization is chosen so that all radial distribution functions approach 1 at infinity.

lated 883.8 ± 3.8 kg/m$^3$, experimental 873.6 kg/m$^3$ [39]). This is no surprise, since the liquid density is one of the properties against which the parent rigid benzene model has been parametrized.[26] The density increases with polymer content. For the mixed systems, it is slightly above the experimental density, which was calculated from the data of ref 40 using the formalism of ref 41. For pure amorphous polystyrene, it reaches 1024.9 ± 3.6 kg/m$^3$ which is slightly below the range of literature values 1040−1065 kg/m$^3$.[42] Two attempts to increase the density of the pure PS sample by annealing cycles (100 ps at 600 K, followed by cooling to 300 K over 200 ps, once with the normal force field, once using soft-core potentials) have failed. We, therefore, tend to believe that the observed density is the density appropriate for our sample of PS, which contains pockets of free volume which cannot relax out. The observed density maximum at 84.6 wt % PS is in line with this notion. Because of their higher mobility, benzene molecules can diffuse into existing cavities. They will first fill them before a volume increase becomes necessary to make room for more benzene.

The isothermal compressibility $\kappa$ was calculated from the fluctuations of the volume $V$ of the simulation cell[33]

$$\langle \delta V^2 \rangle_{NPT} = V k_B T \kappa$$

where $k_B$ denotes Boltzmann's constant. The compressibility for benzene−PS mixtures is shown in Figure 3. Good agreement with experiment is found for the compressibility of pure benzene ($0.97 \times 10^{-10}$ Pa$^{-1}$).[39] With increasing polymer content, the compressibility is approximately constant. If anything, there is a small decrease in the compressibility. This leads to disagreement of the compressibility of pure amorphous polystyrene, for which we find a value of around $0.5 \times 10^{-10}$ Pa$^{-1}$, whereas the experimental value is $2.2 \times 10^{-10}$ Pa$^{-1}$.[42] Even though the compressibility calculated via volume fluctuations is a slowly converging quantity, the observed disagreement can probably not be ascribed to insufficient sampling. We have monitored the evolution of the compressibility with simulation time and have accumulated statistics only after it had converged, which usually was the case at the same time the density had become constant. The discrepancy could be due either to the force field (although the good agreement for neat benzene makes this less likely) or to the particular polystyrene configuration whose compressibility happens to be smaller than the experimental value or to the fact that during a several-nanosecond simulation our PS sample does not sample all possible volume fluctuations. The last possibility would make the calculated $\kappa$ a high-frequency limit, not necessarily equal to the static value. Only much longer simulations with many different polystyrene starting structures could clarify this point. These were not undertaken due to the computational cost. With the limitation of being based on a single amorphous polymer structure only, the calculation of the compressibility (and the related bulk modulus) reduces to an order-of-magnitude estimate. In view of this, we refrain from trying to estimate other elastic constants from fluctuations of geometric parameters of the simulation cell.[43]

**3.2. Polymer and Solvent Structure.** The calculated center-of-mass radial distribution function (RDF) for neat benzene (not shown) is indistinguishable from that of the parent rigid model,[26] this in spite of the different treatment of nonbonded forces (1.0 nm atom−atom cutoff with reaction-field correction vs 1.3 nm molecule−molecule cutoff in the original). The benzene−benzene RDF does not change qualitatively with the polystyrene content (Figure 4). The differing absolute peak heights only reflect different benzene number densities. The mixed benzene−phenyl RDF describes the solvation of the phenyl groups of PS. It is qualitatively very similar to the benzene−benzene RDF. The phenyl−phenyl RDF shows two major differences from the other two. Firstly, there is a small shoulder at around 0.4 nm. This arises from phenyl groups belonging to consecutive monomers. The quadrupole−quadrupole interactions of benzene and phenyl normally lead to a T-shaped arrangement of nearest neighbors, which causes the first peak of the RDF to lie at 0.55 nm. Two consecutive phenyl groups in PS, however, are tied together by the polymer backbone and are forced to approach each other more closely. At the close distance of 0.4 nm they have to assume a coplanar configuration. The second feature in the phenyl−phenyl RDF is the minimum following the first peak (≈0.75 nm). This minimum is not as deep as in the other two RDFs. In fact, it is comparable in height to the second peak of the RDF. Again, the connectivity of the chain enforces distances on pairs of phenyl groups that in a liquid would be unfavorable.

**Table 3. Composition of Nearest-Neighbor Solvent Shells of Benzene Molecules and Phenyl Groups, Respectively[a]**

| wt % polystyrene | no. of benzene molecules | no. of phenyl groups | total no. of neighbors (benzene + phenyl) | benzene/phenyl ratio (in solvation shell) | benzene/phenyl ratio (overall) |
|---|---|---|---|---|---|
| | | (a) Nearest Neighbors of Benzene | | | |
| 0 | 12.6 | 0 | 12.6 | ∞ | ∞ |
| 38.6 | 9.7 | 2.8 | 12.5 | 3.42 | 2.12 |
| 55.7 | 8.4 | 4.4 | 12.7 | 1.92 | 1.06 |
| 72.7 | 5.9 | 6.5 | 12.4 | 0.91 | 0.5 |
| 84.2 | 4.8 | 7.5 | 12.3 | 0.64 | 0.25 |
| | | (b) Nearest Neighbors of Phenyl | | | |
| 38.6 | 6.0 | 5.9 | 11.9 | 1.01 | 2.12 |
| 55.7 | 4.6 | 7.6 | 12.2 | 0.61 | 1.06 |
| 72.7 | 3.3 | 8.5 | 11.7 | 0.38 | 0.5 |
| 84.2 | 1.9 | 9.5 | 11.3 | 0.20 | 0.25 |
| 100 | 0 | 10.8 | 10.8 | 0 | 0 |

[a] Numbers are calculated by integrating the first peak of the appropriate center-of-mass radial distribution function, that is from 0 to 0.75 nm.

It is interesting to compare the composition of the immediate surroundings of a benzene molecule or a phenyl group for the different systems. To this end, we have integrated the first peak of the appropriate RDFs (0−0.75 nm) to obtain the number of each species in the first solvation shell (Table 3). We note that the total number of nearest neighbors of a benzene molecule (Table 3a) is around 12.5 and is practically independent of polymer concentration. As the polymer concentration increases, neighboring benzene molecules are simply replaced by phenyl groups. In contrast, the total number of nearest neighbors of a phenyl group (Table 3b) decreases almost uniformly from 11.9 neighbors (38.6 wt %) to 10.8 neighbors (pure PS). This means, that the connectivity of PS causes aromatic rings to pack less tightly than they would in a liquid. This corroborates the finding of the previous section that pure PS forms a comparatively loose structure and that benzene molecules will find some empty space to fill, before a volume increase is necessary.

From Table 3, it can also be seen that there is some preference for phenyl groups or benzene molecules to be surrounded by like groups or molecules. E.g., at a concentration of 55.7 wt % PS, a phenyl group has, on average, 4.6 benzene molecules in its first solvation shell and 7.6 other phenyl groups. At this composition, the number of phenyl groups and benzene molecules is almost equal, so one would expect a 1:1 ratio of both species, if solvation were purely statistical. In our view, the preference for a like partner can be understood in terms of polymer connectivity. Because of the connectivity, a phenyl group will always have a small number of other phenyls in its first solvation shell. The remaining coordination sites can then be filled statistically. If this hypothesis is true, then the number of predetermined (by the connectivity) neighbors will be (i) independent of concentration, since we always have the same polystyrene chain, and (ii) around 2, since the two adjacent phenyl groups will most likely be inside the first solvation shell. From the data of Table 3, one can calculate the number of predetermined phenyl neighbors of a phenyl group: 3.09, 3.19, 1.99, and 1.97 for 38.6, 55.7, 72.7, and 84.2 wt % PS, respectively. Our data base is too small to determine unambiguously whether there is a trend for this number to decrease from 3 to 2 as one goes to higher polymer concentration, or whether this is merely a coincidence. However, we can conclude that if there are effects other than connectivity that cause nonstatistical solvation, they must be very small indeed.

One can also take a closer look at the mutual orientation of aromatic rings. A convenient measure is the cosine of the angle between the plane normals $\mathbf{u}_3$ of two rings. Because we do not want to distinguish between two symmetrically equivalent orientations (one ring turned by 180°), we use the absolute value of the scalar product $|\mathbf{u}_{3,i}\mathbf{u}_{3,j}|$. This is 1 for two coplanar rings, 0 for a T-shaped arrangement, and $^1/_2$ for a random distribution of orientations. In Figure 5, we show this orientational distribution function (ODF) as a function of the average distance between the pair of rings. For all ODFs, we see that, at a close distance (<0.5 nm), rings are predominantly coplanar. However, one has to keep in mind that there are only very few pairs at this distance, as is evident from the RDFs. We generally observe that orientational correlation is quickly lost with distance, little structure being visible beyond 0.9 nm (this is *before* the second peak in the radial distribution function (Figure 4)). Around the typical nearest-neighbor distance of 0.5 nm, we find minima (below $^1/_2$) which confirm the dominance of perpendicular arrangements in the first solvent shell. For the benzene−benzene and benzene−phenyl ODFs, there is a clear tendency for this minimum to decrease with polymer content. This means that the T-shaped packing of benzene molecules and of benzene molecules around a phenyl group becomes more favored as the polymer content increases. The phenyl−phenyl ODFs are different from the other two, in that there are no minima in the range of the first solvent shell. This indicates that, already at this distance, phenyl groups are randomly oriented. Again, we suspect that connectivity imposes mutual orientation on phenyl rings and that there seems to be no preferred orientation.

**3.3. Benzene Translational Diffusion.** Since the parent benzene model was developed for Monte Carlo use,[26] translational diffusion coefficients have apparently not been calculated. Using a simulation of 215 molecules, we find a self-diffusion coefficient for neat benzene of $1.14\times10^{-5}$ cm$^2$/s compared to experimental values of around $(2.2-2.3)\times10^{-5}$ cm$^2$/s (Table 3[44,45]). Such an agreement, which is not untypical for a well-chosen liquid force field, was deemed sufficient for our purposes.

Benzene diffusion coefficients for all systems are reported in Table 4. As expected, the diffusion coefficient decreases with increasing polymer content. The standard deviation between the Cartesian components of the diffusion coefficient is taken as an imprecision estimate and is given in parentheses. (For a completely

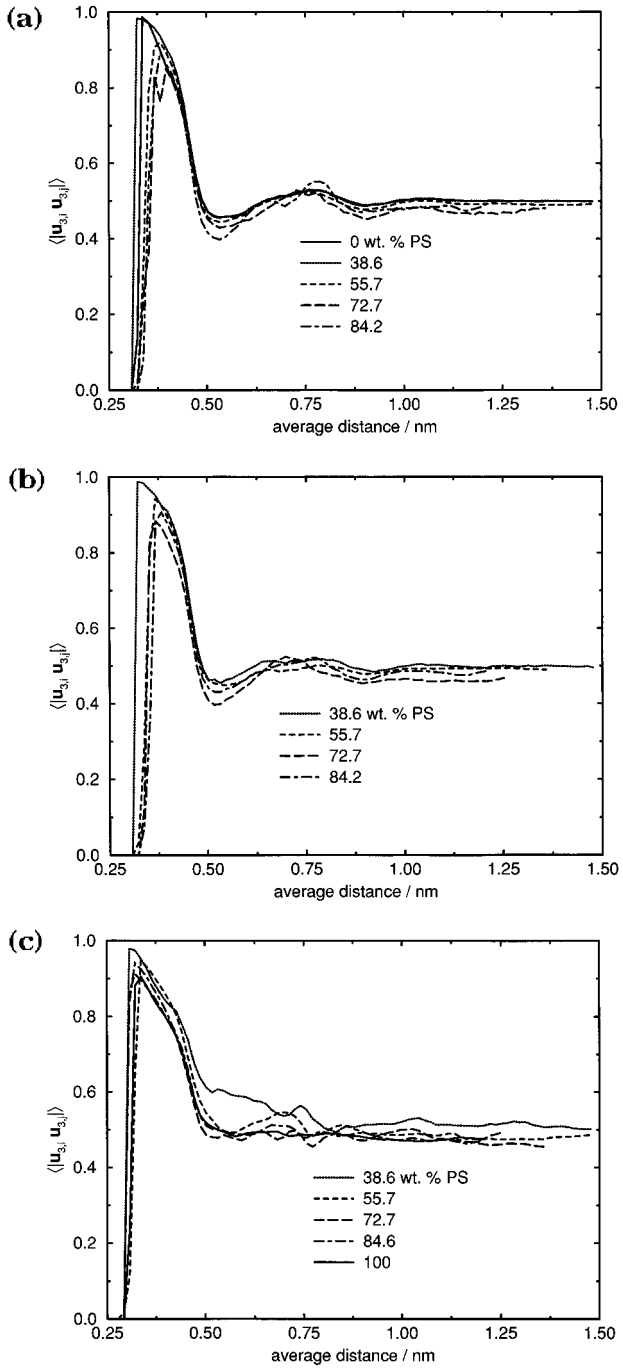


**Figure 5.** Orientation distribution functions describing the mutual orientation of the plane normals of aromatic rings: (a) benzene−benzene; (b) benzene−phenyl; (c) phenyl−phenyl. A value of 1 indicates coplanarity, a value of 0 perpendicular orientation (T shape), a value of $^1/_2$ a random distribution of mutual orientations.

isotropic system, like a macroscopic sample of a liquid or an amorphous polymer, there is no preferential direction of diffusion. This, however, need not be the case for a system of the size simulated here.) The relative error has a tendency to increase toward higher polymer concentration. This is due to slower diffusion and consequently worse sampling of benzene displacements, as well as to lower statistics due to the smaller number of molecules over which to average. The diffusion coefficient at the highest calculated polymer concentration (84.2 wt %) has to be taken as an upper bound to the true diffusion coefficient, since, in spite of the simulation time of 7.4 ns, the shape of the mean-square-displacement curve (not shown) still indicates anomalous (non-Einstein) diffusion behavior:[38] It is not linear in time but follows some power of the time smaller than 1.

The diffusion coefficients normalized by the one for neat benzene ($D_0$) are shown also in Figure 6. A series of experimental data (pulsed-gradient-spin-echo NMR measurements for benzene in PS at 30 °C[7]) are shown in the same representation for comparison. The temperature in the experiment was slightly higher than in our simulation. However, the normalization by $D_0$ makes both data sets comparable. In absolute terms, the calculated diffusion coefficients are smaller than the experimental ones by a factor of approximately 2. This factor is constant over the concentration range and is practically the same as for neat benzene (see above). Therefore, the calculated relative diffusion coefficients ($D/D_0$) of this work show very good agreement with the experimental data.

The representation of Figure 6 (polymer volume fraction $\Phi$ as the abscissa) has been chosen to highlight the similarity of the results to the predictions of the Mackie−Meares model.[46] This lattice model explains the decrease of the solvent diffusion coefficient with polymer concentration entirely in terms of the increased path length of diffusion (tortuosity), which is caused purely by obstruction due to the polymer. There are no assumptions about energetics. It predicts the relative diffusion coefficient to be

$$\frac{D}{D_0} = \left(\frac{1-\Phi}{1+\Phi}\right)^2$$

Note that the Mackie−Meares model is free of adjustable parameters. Our data seem to fit its predictions very well over the concentration range studied. In Figure 6, we also show that the dependence of the relative diffusion coefficient can be fitted by

$$D/D_0 = \exp(a\Phi^b)$$

Such relationships are found for systems of low concentration of polymer (<10 wt %) and mesoscopic diffusants, for which hydrodynamic theories justify exponents $b$ in the range between 0.5 and 1, in agreement with experiment.[47] As we study higher polymer contents and smaller diffusants, it is not surprising that we find an exponent $b$ of 1.44, well outside this range. This probably indicates that, while the assumptions of the hydrodynamic models no longer hold, the stretched exponential is still flexible enough to provide a numerically successful but physically meaningless fit. Because of the uncertainties in our diffusion coefficients we refrain from analyzing them in terms of more complicated or more phenomenological models like the Enskog theory or free-volume theory.[8,9,48,49]

As pointed out in section 2, the definition of a polymer volume fraction can be ambiguous. In that context, it has often been suggested not just to take the volume occupied by the polymer but to include the first shell of solvent molecules on the grounds that they are strongly bound to the polymer and, therefore, less mobile, which would lead to the polymer *including* its first solvation shell acting as an obstacle to diffusion of the remaining "free" solvent molecules. This picture would imply the existence of slow solvent molecules on the polymer surface and fast unbound solvent molecules. Molecular dynamics allows us to test this hypothesis for the present system. In an ever-changing and exchanging

**Table 4. Benzene Diffusion Coefficients and Reorientation Times for Benzene−Polystyrene Systems of Various Compositions at 300 K and 101.3 kPa[a]**

| wt % polystyrene | $D$/cm$^2$ s$^{-1}$ | $\tau_1$/ps (in plane) | $\beta_1$ | $\tau_3$/ps (plane normal) | $\beta_3$ |
|---|---|---|---|---|---|
| 0 | $1.14(0.03) \times 10^{-5}$ (exp $\approx 2.2 \times 10^{-5}$)[b] | 3.05 (exp $\approx$ 2.85)[d] | 0.96 | 4.94 (exp $\approx$ 5.95)[c] | 0.86 |
| 38.6 | $2.99(0.27) \times 10^{-6}$ | 3.96 | 0.90 | 15.1 | 0.61 |
| 55.7 | $4.90(0.74) \times 10^{-7}$ | 5.00 | 0.86 | 39.9 | 0.52 |
| 72.7 | $2.53(0.85) \times 10^{-7}$ | 5.48 | 0.72 | 855 | 0.39 |
| 84.2 | $7.77(0.56) \times 10^{-8}$ | 5.28 | 0.83 | 1228 | 0.35 |
| $\approx$100 | (exp $5.0 \times 10^{-13}$)[c] | | | | |

[a] The values in parentheses denote the standard deviation between the three diagonal components of the diffusion tensor. Also given are the best-fit Kohlrausch exponents $\beta$ for the correlation function for molecular reorientation. [b] References 39 and 42. [c] Reference 6. [d] These values have been calculated as the median of $\tau$ values obtained from a compilation[50] of experimental rotational diffusion constants $D_R = 1/2\tau$ assuming Debye behavior. Measured values of $\tau_1$ range from 0.83 to 9.6 ps (interquartile range 1.8−4.6 ps), values of $\tau_3$, from 1.5 to 9.3 ps (interquartile range 3.5−8.5 ps).

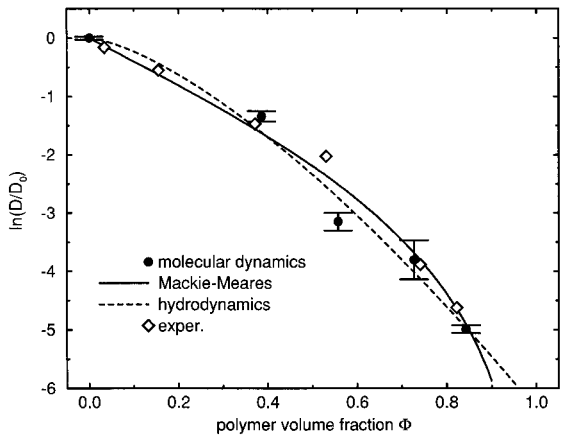


**Figure 6.** Dependence of the diffusion coefficient of benzene in polystyrene on the polystyrene volume fraction. The calculated diffusion coefficients (solid circles) are normalized by the calculated self-diffusion coefficient of pure benzene $D_0$. Also indicated are predictions by the Mackie−Meares model (solid line), a fit to a form from hydrodynamic theory (dashed line), and a series of experimental results on benzene in PS at 30 °C, measured by pulsed-gradient-spin-echo NMR[7] (open diamonds).

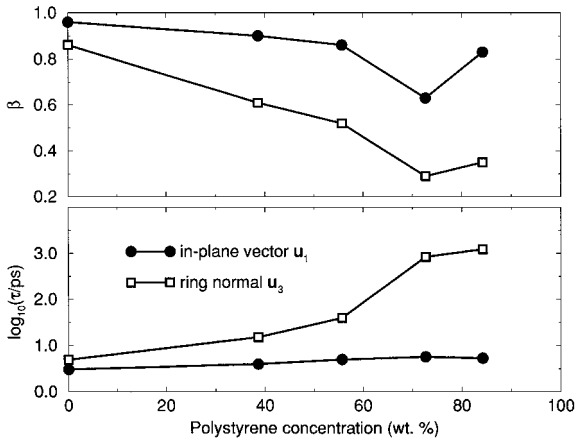


**Figure 7.** Dependence of the benzene reorientation kinetics on the concentration of polystyrene. The correlation times $\tau$ and the Kohlrausch exponents $\beta$ are shown for the reorientation of the in-plane vector $\mathbf{u}_1$ (spinning) and the ring normal $\mathbf{u}_3$ (tumbling).

system, it is impossible to characterize the mobility of individual solvent molecules by something like a local diffusion coefficient. First of all, diffusion takes molecules from one local environment to another. Secondly, bound and unbound molecules can change places. And thirdly, the polymer is mobile, too, and will alter environments quickly. We have resorted to looking at the exchange rates (or rather residence times) of solvent molecules. We define two solvent molecules (or a solvent molecule and a PS phenyl group) to be a contact pair, if their centers of mass are within 0.7 nm of each other; radial distribution functions (cf. Figure 4) indicate that this distance includes the first solvation shell. Then we find out the lifetime for every contact pair and accumulate statistics of these lifetimes. For the 38.6 wt % system, the average lifetime of a benzene−benzene pair is 10.5 ps (standard deviation 34.0 ps), while the average lifetime of a phenyl−benzene pair is 10.3 ps (43.2 ps). In other words, there is no significant difference between the rates with which benzene molecules or phenyl groups replace a member of their first solvation shells. The corresponding lifetime for pure benzene is 8.6 ps (19.7 ps). We can conclude that, while the introduction of polymer slows down the exchange of solvent molecules (and their diffusion), there is no evidence for a separation of time scales for bound and unbound benzene molecules. The present system, however, has only van-der-Waals and quadrupole−quadrupole interactions between polymer and solvent. It cannot be ruled out that systems with particularly strong polymer−solvent interactions (e.g. hydrogen bonds or salt bridges) do show a separation into fast unbound and slow bound solvent fractions.

**3.4. Benzene Reorientation.** The correlation times for the rotation of benzene molecules calculated as described in section 2 are also listed in Table 4. Both correlation times have been measured for neat benzene by various experimental methods (for a compilation, see ref 50). There is a considerable scatter (factor of 10) among the experimental values. Our calculated values fall in the middle of the respective ranges of measured correlation times. The reorientational anisotropy $\tau_3/\tau_1$ is calculated to be 1.62, close to the median of experimental ratios of 1.95 (lowest, 0.55; highest, 6.2; interquartile range, 0.96−2.7). The calculated anisotropy is also in line with a more recent NMR study[51] which found a $\tau_3/\tau_1$ of 1.55.

We find that for both types of motion, reorientation of the in-plane vectors $\mathbf{u}_1$ as well as of the plane normal $\mathbf{u}_3$, the correlation time increases with polymer content. This is intuitively understood, since the polymer generally slows down all benzene motion. At first sight it is, however, quite surprising that the effect is so dramatically different for the two vectors. The correlation time $\tau_1$ for in-plane reorientation increases slowly and by less than a factor of 2 over the whole concentration range, whereas the reorientation time for the ring normal $\tau_3$ increases by almost 3 orders of magnitude toward the largest polymer concentration (see also Figure 7). The difference is, however, easily explained by the geometry of the benzene molecule. It is essentially a flat circular disk. In-plane rotation by as little as 60° brings the molecule to a symmetrically equivalent position. Hence,

there is only very little activation energy (or additional free volume) needed to heave a molecule over a transition state, even if the shape of the cavity it resides in is practically frozen in. In contrast, a reorientation of the plane normal involves tilting the molecule. This needs a substantial deformation of the cavity holding it. Such deformations become more difficult when a large polymer content restricts the general mobility.

It is well possible that the reorientation of $\mathbf{u}_3$ is facilitated by the same mechanism as solvent diffusion. The products of $D$ and $\tau_3$ (Table 4) for the different systems are, from low to high polymer content (in units of $10^{-17}$ cm$^2$), 5.6, 4.5, 2.0, 22, and 9.5. This variation has to be considered small compared to the variation in both factors. Moreover, there is no visible trend, and these values appear to scatter randomly around a mean value of 8.7. We have, therefore, phenomenological evidence that polymer-induced slowing down of translational diffusion and of reorientation of the benzene plane follows the same rules, whereas that of the in-plane reorientation certainly does not.

There are several experimental studies on the reorientation of small molecules inside polymers or gels (see also refs 14 and 52). However, most of the systems are too different from the one studied here to be directly comparable. A depolarized Rayleigh scattering investigation of $CS_2$ in PS (0−100%) concluded that $CS_2$ dominates the dynamics of the mixture for all but the highest polymer concentrations.[3] Fluorescence anisotropy decay measurements of an organic dye in water-swollen poly(acryl amide) found rotational correlation times to increase by about 1 order of magnitude going from pure solvent to a polymer content of about 10 wt %.[4] Depolarized light scattering in mixtures of chlorobenzene and poly(methyl methacrylate) (PMMA) revealed a fast and a slow component of chlorobenzene reorientation,[53] whose concentration dependence did, however, not exhibit the strong disparity found in this work. Another experiment[11] studied, by deuterium NMR, the reorientation of two molecular axes of toluene molecules in neat toluene above and below the glass transition temperature. The ratio between the two modes found there was smaller (factor 1.4−1.8) than that found in our work. Both chlorobenzene and the toluene have symmetries much reduced with respect to that of benzene, so a change in cavity shape is necessary to accommodate the chlorine or the methyl group in the new position also after a spinning motion. This means that both in-plane and normal reorientation would be subject to the same impedance, leading to similar dependence on the polymer concentration. Toluene−PMMA systems were investigated by polarized and depolarized light scattering.[54] There, the toluene reorientational correlation times increased exponentially with PMMA concentration, just like $\tau_3$ of this work. A similar dependence was reported for the reorientation of Aroclor 1248 in PS.[55] NMR measurements of the reorientation of tetrahydrofuran in PS show significant broadening of the distribution of rotational time constants in systems with more than 50% PS.[56] The strongest experimental support for our results comes from a combined depolarized Rayleigh scattering and NMR study of benzene in solvents of different viscosities.[57] There, the $\tau_3$ correlation time was found to increase by 3.5 ps for every increase of the viscosity by 1 cP. We can summarize that for the $\tau_3$ correlation time we find a dependence on polymer concentration similar to what is observed experimentally for analogous systems. What makes benzene a special rotational probe is that its in-plane reorientation time $\tau_1$ is virtually concentration independent, due to its high symmetry.

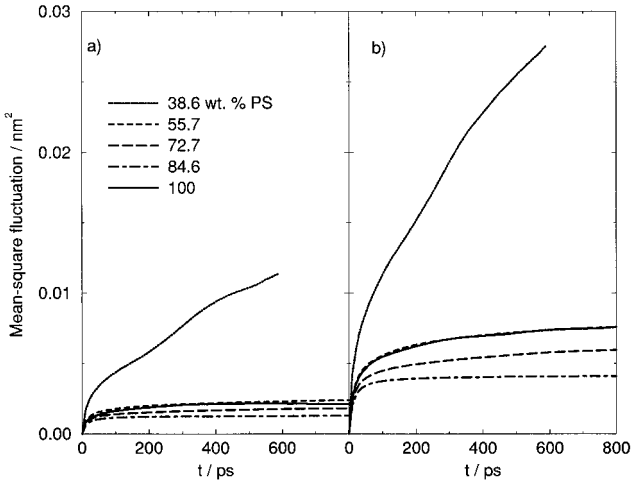


**Figure 8.** Mean-square fluctuation for (a) polystyrene backbone carbon atoms $C_a$ and $C_b$ and (b) para carbon atoms $C_4$ of the pendent phenyl groups.

Together with the correlation times, we display the best-fit Kohlrausch exponents $\beta$ for all systems (Figure 7). A $\beta$ of 1 would indicate exponential reorientation, the hallmark of Debye rotational diffusion.[58] This is found only for the in-plane rotation of pure benzene (the small deviation, $\beta = 0.96$ rather than $\beta = 1$, is probably a fitting error). In all other cases, however, $\beta$ is significantly smaller than 1, meaning that these systems are far from normal rotational diffusion. They do not undergo random jumps in their orientation vectors but, rather, are restricted in their freedom of motion. It is no surprise that $\beta$ moves further away from 1 at higher polymer content and that $\beta_3$ (ring-normal reorientation) is affected more strongly than $\beta_1$ (in-plane reorientation).

**3.5. Polystyrene Dynamics.** The relaxation times of large-scale rearrangements of bulk polymers are much longer than the simulation times of this work. Hence, we can only expect to extract information about local polymer dynamics from our simulation. A convenient measure of atom mobility is the mean-square fluctuation (section 2). This quantity depends on the time over which the averages are performed, and its shape carries the signature of the underlying process. For a diffusing atom, the mean-square fluctuation increases with time, whereas, for a stationary atom, it becomes constant after a certain period. Both situations are clearly visible in Figure 8. For the lowest PS concentration (38.6 wt %), we find a behavior which is essentially diffusive. In 600 ps, a root-mean square fluctuation of about 0.1 nm is achieved for the backbone carbon atoms, and 0.17 nm for the less restricted outer carbons of the phenyl groups. The bent shape of the curves, however, indicates clearly that diffusion is anomalous on this time scale, i.e. that these atoms are not free to perform random motion. At all other compositions, we find the mean-square fluctuation to quickly approach a plateau value, indicating that diffusion is so slow that the structures appear to be static on the time scale of nanoseconds. For both types of atoms, we find that the fluctuations decrease with polymer concentration. This is microscopic evidence for the system becoming stiffer as solvent is removed. The fluctuations for pure polystyrene, however, increase

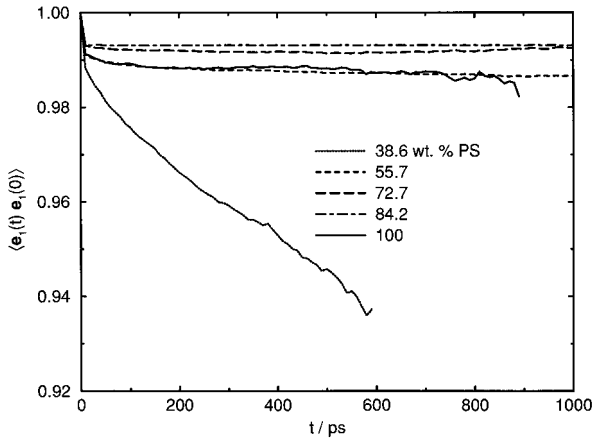


**Figure 9.** Time correlation function $\langle \mathbf{e}_1(t)\mathbf{e}_1(0)\rangle$ for unit vectors between $C_b$ atoms of adjacent styrene monomers.

again and are very similar to the fluctuations of the system with 55.7 wt % PS. This unexpected finding is yet more evidence for the fact that pure polystyrene contains more free volume than benzene−PS mixtures. And it is the free volume which facilitates the fluctuations.

The internal dynamics can be studied also via other quantities. Often the rate of dihedral angle transitions is used to characterize polymer flexibility. In the present case, however, these rates depend little on the system composition (in marked contrast to polymer electrolytes where the salt acts at the same time as a solvent and as an antiplasticizer for the polymer[19]). Transition events are too rare to allow the use of a detailed analysis via time correlation functions.[19] We can obtain, however, rough estimates by simply counting the dihedral angle transitions. Every crossing of the gauche−trans barrier (±120°) is counted as a transition. The period of 1 ps at which configurations are compared suppresses counting of spurious transitions arising from fast recrossing events. On average, a backbone dihedral angle undergoes 1.9 transitions/ns between the trans and the two gauche conformations. The flips of phenyl groups are even rarer: 0.072 $ns^{-1}$. Closer analysis shows that, particularly for the phenyl rotations, these averages arise from very uneven contributions by different monomers. While most monomers show no transitions whatsoever, there are very few monomers locked by packing into conformations near the barrier. Such monomers can cross the barrier back and forth at a much higher rate (every few dozens of picoseconds).

One also can define vectors connecting different monomers. We employ unit vectors denoted $\mathbf{e}_k$ pointing from atom $C_b$ of monomer $i$ to $C_b$ of monomer $i + k$. The time evolution of these vectors can be studied by the same treatment used to study the reorientation of benzene. In Figure 9, we show the correlation functions for the vectors $\mathbf{e}_1$, which connect consecutive monomers. These are expected to show the fastest relaxation and the best statistics. We find again that the system of 38.4 wt % PS sticks out. Here the correlation function shows a visible decay. Extrapolating it by a KWW function and integrating gives a rough guess at the correlation time of 200 ns. At the higher polymer concentrations, the correlation functions show an initial drop (due to vibrational motion) and then become constant. Fitting and integration are not possible. We have also calculated time correlation functions of higher $\mathbf{e}_k$ and have found a qualitatively very similar behavior (not shown). We may conclude that also for this descriptor of polymer motion, the system with the highest solvent content is found to show appreciable, if slow, motion, whereas at all solvent contents of less than 50% the polymer chain is rigid on a nanosecond time scale.

## 4. Summary

We have reported molecular dynamics simulations of a realistic polymer−solvent gel over a wide range of composition (0−84.2 wt % polymer) at atomistic detail. It has been demonstrated that molecular dynamics simulations are capable of describing correctly the structural and dynamical properties of such systems.

We have calculated solvent diffusion coefficients and have found that their composition dependence not only shows reasonable agreement with experiment but that it can also be described quite well by Mackie−Meares theory. It has also been shown that, at least for the polystyrene−benzene system studied here, it is not possible to separate solvent molecules into slow ones, bound to the polymer and traveling with it, and fast ones, not bound to the polymer. This would suggest the polymer chains alone act as obstacles to solvent diffusion and not polymer decorated by a shell of solvent molecules. We have found the reorientation of benzene molecules to be nonexponential and anisotropic, the reorientation of the ring normal being slower than the in-plane reorientation. This anisotropy increases dramatically with polystyrene concentration, an observation supported by experimental observations of analogous polymer−solvent systems as well as liquid mixtures. At the highest polymer concentration, the time scales for the two motions are separated by 3 orders of magnitude. There is evidence that the reorientation of the ring normal is affected by the same influences as the translational diffusion, while the in-plane reorientation is not.

The microscopic polymer dynamics in benzene−polystyrene mixtures depends strongly on the solvent content. For a solvent content above 50%, we find the polymer motion to be diffusive in nature. At lower solvent concentrations, the polymer structure is essentially rigid on a nanosecond time scale, with only local fluctuations being possible. Polymer diffusion may, of course, still take place at longer time scales.

**Acknowledgment.** It is a pleasure to acknowledge W. F. van Gunsteren for helpful discussions and perusal of the manuscript. I also thank Mark D. Ediger (University of Wisconsin) for pointing out important references. This work has been made possible by generous allocations of supercomputer time by Cray Research, Inc. and the ETH Computer Centre.

## References and Notes

(1) Kreibich, U. T.; Schmid, R. In *Polymere Werkstoffe*; Batzer, H., Ed.; Thieme: Stuttgart, 1985.
(2) Ono, K.; Okada, Y.; Yokotsuka, S.; Sasaki, T.; Yamamoto, M. *Macromolecules* **1994**, *27*, 6482.
(3) Pesce da Silveira, N.; Stassen, H.; Dorfmüller, Th. *J. Chem. Phys.* **1995**, *101*, 9370.
(4) Mikosch, W.; Dorfmüller, Th.; Eimer, W. *J. Chem. Phys.* **1994**, *101*, 11052.
(5) Rizos, A. K.; Johnsen, R. M.; Brown, W.; Ngai, K. L. *Macromolecules* **1995**, *28*, 5450.
(6) Berens, A. R.; Hopfenberg, H. B. *J. Membr. Sci.* **1983**, *10*, 283.
(7) Kosfeld, R.; Goffloo, K. *Kolloid Z. Z. Polym.* **1971**, *247*, 801.
(8) Pickup, S.; Blum, F. D. *Macromolecules* **1989**, *22*, 3961.

(9) Waggoner, R. A.; Blum, F. D.; MacElroy, J. M. D. *Macromolecules* **1993**, *26*, 6841.
(10) Ilyina, E.; Sillescu, H. *Polymer* **1995**, *36*, 137.
(11) Hinze, G.; Sillescu, H.; Fujara, F. *Chem. Phys. Lett.* **1995**, *232*, 154.
(12) Fytas, G.; Rizos, A.; Floudas, G.; Lodge, T. P. *J. Chem. Phys.* **1990**, *93*, 5096.
(13) Rizos, A.; Fytas, G.; Lodge, T. P.; Ngai, K. L. *J. Chem. Phys.* **1991**, *95*, 2980.
(14) Müller-Plathe, F. *Acta Polym.* **1994**, *45*, 259.
(15) Gusev, A. A.; Müller-Plathe, F.; van Gunsteren, W. F.; Suter, U. W. *Adv. Polym. Sci.* **1994**, *116*, 207.
(16) Tamai, Y.; Tanaka, H.; Nakanishi, K. *Macromolecules* **1994**, *27*, 4498.
(17) Müller-Plathe, F. *J. Chem. Phys.* **1995**, *103*, 4346.
(18) Neyertz, S.; Thomas, J. O.; Brown, D. *Comput. Polym. Sci.* **1995**, *5*, 107.
(19) Müller-Plathe F.; van Gunsteren, W. F. *J. Chem. Phys.* **1995**, *103*, 4745.
(20) Müller-Plathe, F.; Liu, H.; van Gunsteren, W. F. *Comput. Polym. Sci.* **1995**, *5*, 89.
(21) Depner, M.; Schürmann, B. L. *J. Comput. Chem.* **1992**, *13*, 1210.
(22) Moe, N. E.; Ediger, M. D. *Macromolecules* **1995**, *28*, 2329.
(23) Karlström, G.; Linse, P.; Wallqvist, A.; Jönsson, B. *J. Am. Chem. Soc.* **1983**, *105*, 3777.
(24) Linse, P. *J. Am. Chem. Soc.* **1984**, *106*, 5425.
(25) Linse, P.; Engström, S.; Jönsson, B. *Chem. Phys. Lett.* **1985**, *115*, 95.
(26) Jorgensen, W. L.; Severance, D. L. *J. Am. Chem. Soc.* **1990**, *112*, 4768.
(27) Modello, M.; Yang, H.-J.; Furuya, H.; Roe, R.-J. *Macromolecules* **1994**, *27*, 3566.
(28) Furuya, H.; Modello, M.; Yang, H.-J.; Roe, R.-J.; Erwin, R. W.; Han, C. C.; Smith S. D. *Macromolecules* **1994**, *27*, 5674.
(29) Roe, R.-J.; Modello, M.; Furuya, H.; Yang, H.-J. *Macromolecules* **1995**, *28*, 2807.
(30) Rapold, R. F. Ph.D. Thesis (ETH No. 10308), Swiss Federal Institute of Technology Zürich, 1993.
(31) Rapold, R.; Suter, U. W.; Theodorou, D. N. *Makromol. Chem. Theory. Simul.* **1994**, *3*, 19.
(32) Müller-Plathe, F. *Braz. J. Phys.* **1994**, *24*, 956.
(33) Allen, M. P.; Tildesley, D. J. *Computer Simulation of Liquids*; Oxford Science Publishers: Oxford, U.K., 1987.
(34) Müller-Plathe, F. *Comput. Phys. Commun.* **1993**, *78*, 77.
(35) Berendsen, H. J. C.; Postma, J. P. M.; van Gunsteren, W. F.; Di Nola, A.; Haak, J. R. *J. Chem. Phys.* **1984**, *82*, 3684.
(36) Ryckaert, J.-P.; Ciccotti, G.; Berendsen, H. J. C. *J. Comput. Phys.* **1977**, *23*, 327.
(37) Müller-Plathe, F.; Brown, D. *Comput. Phys. Commun.* **1991**, *64*, 7.
(38) Müller-Plathe, F.; Rogers, S. C.; van Gunsteren, W. F. *Chem. Phys. Lett.* **1992**, *199*, 237.
(39) Lide, D. R., Ed. *Handbook of Chemistry and Physics*, 74th ed.; CRC Press: Boca Raton, FL, 1993.
(40) Sarazin, D.; François, J. *Macromolecules* **1985,** *18*, 1190.
(41) Schulz, G. V.; Hoffmann, M. *Makromol. Chem.* **1957**, *23*, 220.
(42) Brandrup, J., Immergut, E. H., Eds. *Polymer Handbook*, 3rd ed.; Wiley: New York, 1989.
(43) Gusev, A. A.; Zehnder, M. M.; Suter, U. W.; *Macromolecules* **1994**, *27*, 615.
(44) Falcone, D. R.; Douglass, D. C.; McCall, D. W. *J. Phys. Chem.* **1967**, *71*, 2754.
(45) McCool, M. A.; Collings, A. F.; Woolf, L. A. *J. Chem. Soc., Faraday Trans. 1* **1972**, *68*, 1489.
(46) Mackie, J. S.; Meares, P. *Proc. R. Soc. London* **1955**, *A232*, 498.
(47) Ogston, A. G.; Preston, B. N.; Wells, J. D. *Proc. R. Soc. London* **1973**, *A333*, 297. Langevin, D.; Rondelez, F. *Polymer* **1978**, *19*, 875. Cukier, R. I. *Macromolecules* **1984**, *17*, 252. Altenberger, A. R.; Tirrell, M. *J. Chem. Phys.* **1984**, *80*, 2208. Altenberger, A. R.; Tirrell, M.; Dahler, J. S. *J. Chem. Phys.* **1986**, *84*, 5122. Phillies, G. D. J. *Macromolecules* **1987**, *20*, 558; **1988**, *21*, 3101.
(48) Muhr, A. H.; Blanchard, J. M. V. *Polymer* **1982**, *23*, 1012.
(49) Vrentas, J. S.; Vrentas, C. M. *Macromolecules* **1994**, *27*, 4684.
(50) Tanabe, K. *Chem. Phys. Lett.* **1979**, *63*, 43.
(51) Dölle, A.; Suhm, M. A.; Weingärtner, H. *J. Chem. Phys.* **1991**, *94*, 3361.
(52) Müller-Plathe, F.; van Gunsteren, W. F. *Polym. Prepr. (Am. Chem. Soc., Div. Polym. Chem.)* **1992**, *33* (1), 633.
(53) Ouano, A. C.; Pecora, R. *Macromolecules* **1980**, *13*, 1167, 1173.
(54) Floudas, G.; Fytas, G.; Brown, W. *J. Chem. Phys.* **1992**, *96*, 2164.
(55) Lodge, T. P. *J. Phys. Chem.* **1993**, *97*, 1480.
(56) Gisser, D. J.; Johnson, B. S.; Ediger, M. D.; von Meerwall, E. D. *Macromolecules* **1993**, *26*, 512.
(57) Bauer, D. R.; Alms, G. R.; Brauman, J. I.; Pecora, R. *J. Chem. Phys.* **1974**, *61*, 2255.
(58) McQuarrie, D. A. *Statistical Mechanics*; Harper-Collins: New York, 1976.

MA9518767